An optimization tool to design the field of a Solar Power Tower plant allowing heliostats of different sizes

E. Carrizosa[a,b], C. Domínguez-Bravo[c,*], E. Fernández-Cara[d,b], M. Quero[e]

[a]Department of Statistics and Operations Research, University of Seville, Spain
[b]IMUS - Mathematics Institute of the University of Seville, Spain
[c]BCAM - Basque Center for Applied Mathematics, Bilbao, Spain
[d]Department of Differential Equations and Numerical Analysis, University of Seville, Spain
[e]Abengoa Solar New Technologies, Seville, Spain

Abstract

The design of a Solar Power Tower plant involves the optimization of the heliostat field layout. Fields are usually designed to have all heliostats of identical size. Although the use of a single heliostat size has been questioned in the literature, there are no tools to design fields with heliostats of several sizes at the same time.

In this paper, the problem of optimizing the heliostat field layout of a system with heliostats of different sizes is addressed. We present an optimization tool to design solar plants allowing two heliostat sizes. The methodology is illustrated with a particular example considering different heliostat costs.

Keywords: solar thermal power tower, field layout, multi-size-heliostat field, heuristic algorithm, greedy algorithm

1. Introduction

Solar power tower (SPT) system is known as one of the most promising technologies for producing solar electricity due to the high temperatures reached that result in high thermodynamic performances; some reviews on solar thermal electricity technology are [1, 2, 3, 4]. In an SPT system, direct solar radiation is reflected and concentrated by the heliostat field in a receiver placed at the top of the tower. At the receiver, the solar energy is converted into thermal energy by heating a fluid which can be used to generate electricity through a conventional thermodynamic cycle. The heliostat field is composed of a group of mirrors having usually two-axis tracking system to reflect the direct light from the sun to the receiver aperture.

---

[*]BCAM - Basque Center for Applied Mathematics,
Mazarredo, 14 E48009 Bilbao, Basque Country, Spain.
E-mail: cdominguez@bcamath.org

The optimization of the field layout to minimize the levelized cost of energy (LCOE) is a challenging problem due to several reasons: the problem is of very large dimension (with hundreds, or even thousands, of variables), involves non-convex constraints and the objective function is nonsmooth, hard to compute and multimodal [5].

With the purpose of reducing the complexity of the problem, a geometrical pattern is frequently imposed, i.e. the heliostats locations follow a fixed distribution. Usually, a radially-staggered [6, 7, 8, 9, 10], spiral [11] or grid [12] distribution is used. Thus, the heliostat field layout is calculated through the optimization of a low number of parameters defining the geometry of the selected distribution.

Since 1970s, different research programs have been financed to study the heliostat design aiming to break down the heliostat costs while maintaining the collected energy. Original ideas have been developed in recent studies (hexagonal [13], bubble [14], minimirror array [15] and other geometries [16, 17, 18]), see also [19, 20, 21, 22, 23]. Some promising prototypes are the following: the autonomous heliostat (CIEMAT PCHA project [24, 25]), the EASY heliostat (hEliostat for eAsy and Smart deploYment [26]) and the SCS5 eSolar next generation heliostat [27].

The heliostat optical design influences the overall performance of the system (ratio of ground coverage, number of heliostats, receiver size and tower height), and it is influenced by the cost (manufacturing and assembly processes, canting, installation, calibration, etc.), and wind loads among others, see [14, 28, 13, 29, 18]. As pointed out in several studies [14, 21, 26], efficient fields can be designed with large or big heliostats ($148\,m^2$ ATS [14], $121\,m^2$ Sanlucar [30], $116\,m^2$ Sener [21]) but also using small or micro heliostats ($16\,m^2$ AORA Solar and Heliko-DLR [14], $7.5\,m^2$ [31], $4.3\,m^2$ SHP-CSIRO [29]).

As pointed out in [32], the use identical sizes may not lead to optimal fields. Despite this, the design of fields using heliostats of different sizes together remains, as far as the authors are aware of, unexplored.

In this paper we will focus on the optimization of a multi-size-heliostat field (a heliostat field with different heliostat sizes) using a pattern-free method. For simplicity, we will assume that the tower and receiver are fixed (to address the whole optimization problem, see [33]), the pedestal height remains the same for all heliostat sizes and, as usual, all heliostats will be assumed to focus onto the same target point: the aperture centre.

The rest of the paper is organized as follows. In Section 2, we describe the main ingredients affecting the behaviour and performance of the SPT system. Our methodology to solve the optimization problem is explained in Section 3. In Section 4, we present the heliostat sizes used in this paper and we apply the proposed algorithm and analysis tools to a typical plant design. Finally, in Section 5, our main results are summarized and some perspectives for further work are presented.

2. Problem statement

In this section, we explain the meaning of the variables involved in the optimization process. We also present the constraints that have to be satisfied, the cost and energy functions (which are the elements to be considered for the computation of the objective function LCOE), and the optimization problem itself.

2.1. Variables

The heliostats locations, given by the coordinates (x, y) of their centres, and the heliostat sizes d, are the variables to be used. From now on, we will denote by Ω the collections of coordinates of the centres and sizes of the heliostats, namely (x, y, d). The set Ω is described as follows:

$$\Omega = \{(x_i, y_i, d_i) \text{ for } i \in [1, N] \text{ with } (x_i, y_i) \in \mathcal{S} \text{ and } d_i \in \mathcal{D}\}, \tag{1}$$

where N denotes the total number of heliostats, $\mathcal{S}$ is the set of heliostats coordinates and $\mathcal{D}$ is the set of heliostat sizes. We assume that the set $\mathcal{D}$ is finite.

For simplicity, all heliostats are assumed to be rectangular and have the same pedestal height, although they can have different dimensions. Note that these assumptions help to reduce the computation of the shading and blocking effects caused by large-size heliostats on the smaller ones.

2.2. Constraints

Usually, when designing an SPT system, a fixed time is used to evaluate the plant operation. This time is known in the literature as the *design point*, denoted here by T_{d}. Let $\Pi_{T_{\mathrm{d}}}(\Omega)$ be the power input obtained at the design point. Then, a minimal power input has to be achieved, that is, the following constraints has to be satisfied:

$$\Pi_{T_{\mathrm{d}}}(\Omega) \geq \Pi_0. \tag{2}$$

Due to technical reasons, the heliostats must be located within a given region $\mathcal{S}_0 \subset \mathbb{R}^2$:

$$\mathcal{S} \subset \mathcal{S}_0. \tag{3}$$

The heliostats located in the field have to rotate freely avoiding collisions with other heliostats. Consequently, we have to include constraints forcing the heliostats not to overlap:

$$||(x, y) - (x', y')|| \geq \delta(d) + \delta(d') \quad \forall (x, y, d), (x', y', d') \in \Omega \text{ with } (x, y) \neq (x', y'), \tag{4}$$

where the radius of the clear-out circle for heliostat size d is $\delta(d) = 0.5 \, diag(d) + 0.5 \, d_{\mathbf{s}}$. Here, $diag(d)$ denotes the heliostat diagonal and $d_{\mathbf{s}}$ is a positive constant, related to installation errors and heliostat accessibility, which remains equal for all the heliostat sizes in this paper.

2.3. Functions

The cost and the annual energy are the functions involved in the objective function. The cost function $C = C(\Omega)$ takes into account the investment in power plant equipment (tower, receiver and heliostat field), purchasing of land and civil engineering costs:

$$C(\Omega) := K + \Psi(\Omega), \text{ with } \Psi(\Omega) := \sum_{d \in \mathcal{D}} c(d) N_d \,, \tag{5}$$

where K is a constant including all fixed costs (independent of the configuration of the heliostat field) and $\Psi(\Omega)$ represents the heliostat field cost function. The number of heliostats of each size is denoted by N_d and $c(d)$ denotes the cost per heliostat of size d. All costs associated with the heliostats (mirror modules, support structure, drives, pedestal, foundation, field wiring, etc.) are included in $c(d)$ and, for simplicity, they are supposed to be independent of the heliostat position.

The annual energy input function $E = E(\Omega)$ takes the form:

$$E(\Omega) := \int_0^T I(t) \sum_{i=1}^N \varphi(t, x_i, y_i, d_i, \Omega) \, dt \,, \tag{6}$$

where $I(t)$ is the so-called instantaneous direct solar radiation and φ represents the product of the heliostat efficiencies (usual in this framework), that is, $\varphi = f_{ref} f_{at} f_{cos} f_{sb} f_{sp}$.

Specifically, f_{ref} is the heliostat reflectance factor, f_{at} is the atmospheric efficiency, [34, 35]; f_{cos} is the cosine efficiency, [35]; f_{sb} is the shading and blocking efficiency [6, 36], and, finally, f_{sp} is the interception efficiency or spillage factor [37].

The annual energy of the plant is computed with a procedure similar to NSPOC (Nevada Solar Power Optimization Code) [38]. We refer the reader to [34, 37, 35] for further details. We have developed a Matlab prototype to adapt the energy calculation when having different heliostat sizes and, in particular, address the shading and blocking effects.

2.4. Optimization Problem

The optimization problem we are addressing can be written as follows:

$$(\mathcal{P}) \begin{cases} \text{Minimize} & F(\Omega) = C(\Omega)/E(\Omega) \\ \text{Subject to} & \Pi_{T_d}(\Omega) \geq \Pi_0 \\ & \Omega \subset \mathcal{S}_0 \times \mathcal{D} \\ & ||(x, y) - (x', y')|| \geq \delta(d) + \delta(d') \quad \text{for } (x, y, d), (x', y', d') \in \Omega \\ & \text{with } (x, y) \neq (x', y') \,. \end{cases} \tag{7}$$

In this problem, the number of heliostats is not fixed in advance. Note that, even fixing this number, the huge amount of heliostats in recent commercial plants makes this problem very difficult to solve, as pointed out in [2].

Some of the heliostat efficiency functions depend on the heliostat area and/or the position in the field (interception efficiency [39, 40, 5], atmospheric efficiency [2, 11], etc.) Hence, the heliostats annual energy per unit area values are different depending on their positions, see Figure 1. These values are similar in general for both sizes although they have a different behaviour in regions below the two quadrant diagonals (due to the interception efficiency, see Figure 2).

3. Field optimization algorithm

The aim of this paper is the field layout design when having different heliostat sizes. The proposed algorithm aims to work with any selected size having arbitrary aspect ratio, cost, etc. We describe our approach in the case of two sizes (big and micro heliostats), but the methodology extends easily to the general case.

The proposed procedure, called *Expansion-Contraction Algorithm*, starts with a large-size heliostat field (calculated following the *Greedy Algorithm* explained in Section 3.1, see also [33, 41]) and complements it by inserting small-size heliostats. Following this algorithm, large-size heliostats will be located at the best positions taking advantage of the most favourable region near the tower. Then, two consecutive phases, called *Expansion* and *Contraction*, are applied and repeated until a stopping condition is fulfilled. At the *Expansion Phase*, small-size heliostats are inserted with the *Greedy Algorithm*. At the *Contraction Phase*, the best heliostats are selected according to their LCOE per unit area values and the worst are sequentially deleted. The *Expansion-Contraction* algorithm is explained in detail in Section 3.2.

In order to allow the possibility of mixed-fields when having big and micro heliostats, the algorithm starts locating big heliostats first. If smaller heliostats were considered as first candidates, only infeasible positions would remain for the location of large heliostats if required. This way, the same idea presented in [42] is followed:
" The best strategy to fill a case with stone, pebble and sand is as follows. First filling the case with the stones and then filling the gap left from the stones with pebbles and in the same way, filling the gap left from pebbles with sand. Since filling in opposite direction may leave the stones or pebbles outside."

3.1. Greedy Algorithm

The procedure presented in this paper makes use of the *Greedy Algorithm*, designed in [33] to calculate a field layout with a single heliostat size. This is a method that sequentially locates the heliostats one by one in the field at the best feasible position. The annual energy values are modified at each step due to the shading and blocking effects that the new heliostat produces in the field.

For simplicity, it is assumed that the heliostat cost is independent of the heliostat location, so that the annual energy function E can be viewed as the objective function. The heliostats are located freely, without any pre-arranged
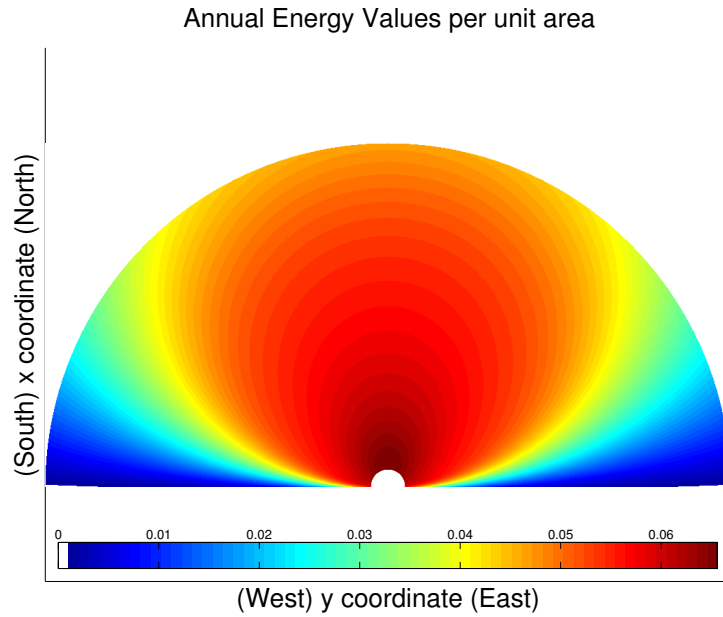
Annual Energy Values per unit area

Figure 1: Annual energy per heliostat unit area of small-size ($GWHth/m^2$). Outer semicircle has a radius of 9.95 tower heights ($1\,km$).
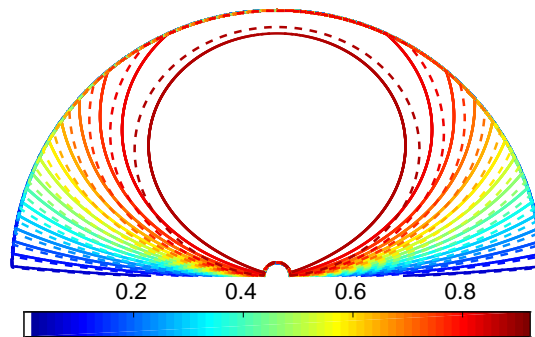
Annual Interception Efficiency Values

Figure 2: Interception efficiency (values in $[0, 1]$), overlapping of small-size (thin lines) and large-size (thick lines) heliostat effects.

distribution. Only two geometrical constraints have to be taken into account: the field shape constraint (3) and the constraints to avoid heliostat collisions (4).

Obviously, the first problem involves locating the first heliostat centre when only the field shape constraint is considered. This problem has an easy-to-handle objective function, because of the absence of shading and blocking effects. In return, when we have already located $k - 1$ heliostats and we have obtained a field $\Omega^{k-1} = \{(x_1, y_1, d_1), \ldots, (x_{k-1}, y_{k-1}, d_{k-1})\}$ that fulfils (3) and (4), the problem $(\mathcal{P}^k)$ described below is difficult to solve, since non-convex constraints are involved and the energy function has a complex shape due to the shading and blocking effects.

Let us introduce the notation $\Omega^k = \Omega^{k-1} \cup \{(x, y, d)\}$, where (x, y) denotes the variables with respect to which we maximize in problem $(\mathcal{P}^k)$. Now, we focus on the problem of finding the optimal location of a new heliostat:

$$\left(\mathcal{P}^k\right) \begin{cases} \text{Maximize} & E(\Omega^{k-1} \cup \{(x, y, d)\}) \\ \text{Subject to} & (x, y) \in \mathcal{S}_0 \\ & ||(x, y) - (x', y')|| \geq \delta(d) + \delta(d') \quad \forall (x', y', d') \in \Omega^{k-1} \,. \end{cases} \tag{8}$$

When $k > 0$, this problem becomes multi-modal due to the shading and blocking effects. A multi-start procedure is used to avoid local minima starting from several randomly selected feasible positions. The final solution is chosen according to the annual energy given by each configuration. The final number of heliostats is given by the algorithm. It stops when the power requirement are reached.

3.2. Expansion-Contraction Algorithm

The *Expansion-Contraction* algorithm starts with a feasible large-size heliostat field that reaches the power input constraint (2) and then makes a series of *Expansion-Contraction* steps. The *Expansion-Contraction* algorithm is described in Algorithm 1.

The *Expansion Phase* consists of oversizing the large-size field using small-size heliostats until a prescribed power input value Π_0^+, greater than Π_0, is reached. The small-size heliostats are located one by one following the *Greedy Algorithm*, recalculating the shading and blocking effects at each step. Small-size heliostats are expected to fill-in possible holes between the large-size heliostats already located due to their smaller area. Moreover, as can be seen in the contour lines shown in Figure 2, they reach higher energy per unit area values in lateral regions.

Once the oversized multi-size-heliostat field is obtained, the heliostats are arranged according to their LCOE per unit area values. At the *Contraction Phase*, the heliostats reaching lowest values are (sequentially) deleted and the number of selected heliostats is determined by (2). This phase has to follow a sequential procedure because once a heliostat is deleted, the shading and blocking effects over its neighbours change and, therefore, their values have to be recalculated. This process can be carried out selecting carefully the active neighbours in order to avoid the recalculation of the annual energy of the whole field and,

consequently, reducing the computational time. Oversizing and selection are well-known in the field layout problem, as they are usually used in combination with some fixed-pattern strategies, see [6, 7, 10, 11].

Algorithm 1 Expansion-Contraction Algorithm

Require: Π_0 and Π_0^+

$\boxed{\Omega_0} \leftarrow \begin{cases} \text{Create initial field using large-size heliostats with } \textit{Greedy Algorithm.} \\ \text{Stop when } \Pi_0 \text{ is reached.} \end{cases}$

$F_0 \leftarrow F(\Omega)$
$\Upsilon_{obj} \leftarrow F_0$
$\Upsilon_{field} \leftarrow \Omega_0$
$stop \leftarrow 0$
$k \leftarrow 0$
while $k \leq k_{max}$ & $stop = 0$ **do**
  Expansion Phase:
  $\boxed{\Omega_k^+} \leftarrow \begin{cases} \text{Oversize } \Omega_k \text{ using small-size heliostats with } \textit{Greedy Algorithm.} \\ \text{Stop when } \Pi_0^+ \text{ is reached.} \end{cases}$

  Contraction Phase:
  $\boxed{\Omega_k^-} \leftarrow \begin{cases} \text{Sort } \Omega_k^+ \text{ according to: LCOE per unit area.} \\ \text{Select the best heliostats until } \Pi_0 \text{ is reached.} \end{cases}$
  Update:
  $k \leftarrow k + 1$
  $F_k \leftarrow F(\Omega_k^-)$
  $\Omega_k \leftarrow \Omega_k^-$
  if $F_k \geq \Upsilon_{obj}$ **then**
      $\Upsilon_{obj} \leftarrow F_k$
      $\Upsilon_{field} \leftarrow \Omega_k$
  else
      $stop \leftarrow 1$
  end if
end while
return $\boxed{\Upsilon_{field}}$

---

4. Results

In our experiments we consider the large-size heliostat of the kind `HLarge`, whose area is $121.34\,m^2$ (similar to the usual heliostat used with the selected tower-receiver configuration, see Table 2, the heliostat Sanlucar120 [30, 43]). The small-size heliostats are of the `HSmall` kind, with area $4.35\,m^2$ (similar to the SCS5 eSolar heliostat [27]). In Table 1 and Figure 3 both are fully described.

Several studies, see [14, 20], support a reduction on the heliostat cost per unit area for small heliostats compared to large heliostats. In this paper, the

heliostat cost per unit area is set to 158.61 $/m^2$ and two different cost scenarios are studied:

- Scenario-100: For small-size and large-size heliostats, the costs per unit area are identical.

- Scenario-80: For small-size heliostats, the cost is only 80%.

The corresponding LCOE functions are respectively denoted F_{100} and F_{80}.

For simplicity, in this paper the pedestal height and safe distance remain the same for all heliostat sizes. These assumptions help to reduce the shading and blocking effects caused by large-size heliostats over the smaller ones. However, note that the selected sizes have different aspect ratio, which implies a different clear-out ratio. Therefore, these effects and the computed solutions will depend strongly on the selected heliostat sizes.

Heliostat Parameter		Large-size	Small-size
Name		HLarge	HSmall
Width	$[m]$	12.84	3.21
Height	$[m]$	9.45	1.36
Optical height z_0	$[m]$	5.17	5.17
Diagonal	$[m]$	15.94	3.49
Safe distance d_s	$[m]$	1.70	1.70
Security distance $\delta(d)$	$[m]$	17.64	5.19
Aspect Ratio (width/height)		1.36	2.36
Total Area A_d	$[m^2]$	121.34	4.35
Relative Area		1	0.25
Hel. Cost Scenario-100	$[\$/m^2]$	158.61	158.61
Hel. Cost Scenario-80	$[\$/m^2]$	158.61	126.89

Table 1: Parameter Values (Heliostat sizes)

In view of the tower parameters detailed in Table 2, we see that the maximum thermal energy value is reached at coordinates $(74.41, 0)$, i.e., 0.74 tower heights to the North. Note that this value belongs to the interval $[0.5, 1]$, given in [8]. Therefore, as can also be appreciated in Figure 1, this region (near the tower) is in principle the most favourable to locate heliostats and a higher density of heliostats is expected there, as pointed out in [11, 29].

The annual energy per unit area generated by one single heliostat is very similar for both sizes in general. However, the interception efficiency values differ, specially in regions below the two quadrant diagonals, and furnish better results with the small-size heliostat (thick lines in Figure 2).

The *Expansion-Contraction Algorithm* described in Section 3.2 has been implemented in Matlab$^©$, using the `fmincon` routine to solve the involved optimization subproblems. The specific values for the receiver-field parameters are shown in Table 2.

The power input required at the design point Π_0 is set to 45.03 MWth. The value for the upper limit Π_0^+ is set to 49.51 MWth (an increase of 10%
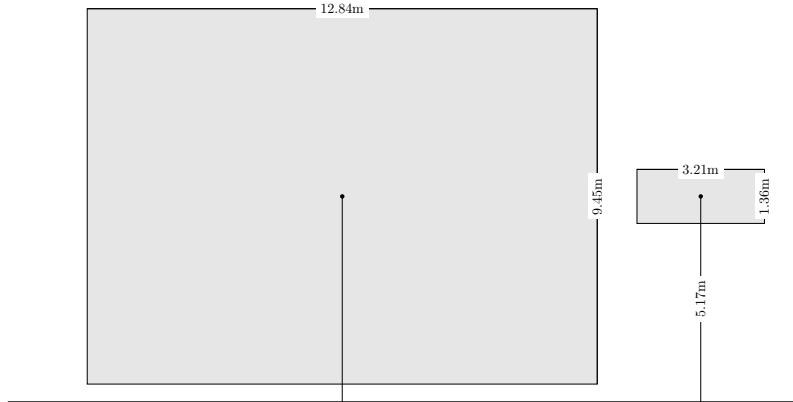
Figure 3: `HLarge` and `HSmall`

Parameter	Default value	Reference
Location and Time		
Emplacement	Sanlúcar la Mayor (Seville)	[44]
Latitude	$37^o26'$ N	[11]
Longitude	$6^o15'$ W	[11]
Design Point T_{d}	March 21 Day 12 Hour	assumed
Design direct normal irradiation DNI	823.9 W/m^2	assumed
DNI model	cloudless skies	assumed
Tower and Receiver		
Tower optical height h	100.50 m	[11]
Aperture radius r_a	6.39 m	assumed
Aperture slope ξ	12.5	[11]
Minimum radius of the field	50 m	assumed
Thermal receiver minimal power input at T_{d}	45.03 MWth	assumed
Field		
Slope	0°	assumed
Feasible region shape	annulus	assumed
Maximum size	156.68 ha	assumed

Table 2: Parameter Values (Receiver and Field)

on Π_0). In order to compare our results, we use a reference system similar to the **PS10** configuration but achieving Π_0 and called **PS10**-592, similar to a solar commercial plant located in Seville, see Figure 4(a). The initial field Ω_0, see Figure 4(b), is obtained with the *Greedy Algorithm* considering the power requirements Π_0. Note that any heliostat field could be used instead, multi-size or single-size.

Let us also mention that our approach does not impose a priori any prescribed or preferred location for heliostats of a given (small or large) size. Contrarily, we try to leave this completely free. As detailed in Table 2 and Figure 1, the feasible region has an annulus shape. However, note that in the following examples the heliostats are located by the algorithm automatically at the north area, where higher energy values are reached.
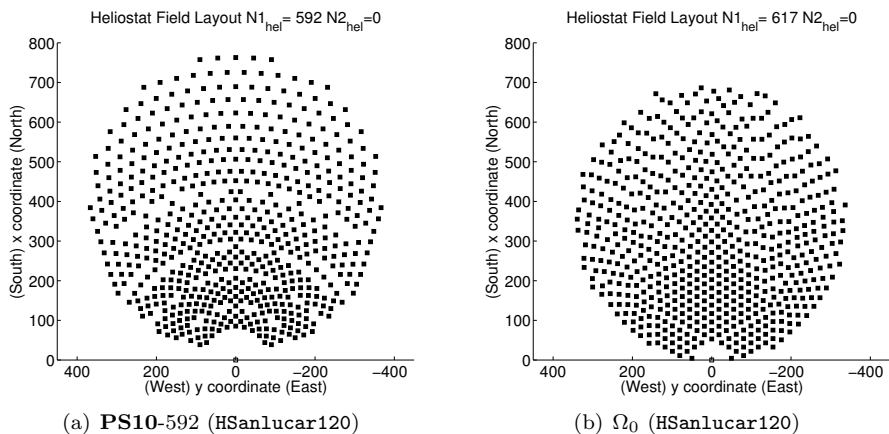

(a) **PS10**-592 (`HSanlucar120`)   (b) Ω_0 (`HSanlucar120`)

Figure 4: **PS10**-592 and Ω_0

Two different cost scenarios are studied, called Scenario-100 and Scenario-80. In Figure 5, the contraction step of Ω_0 is detailed for both cost scenarios. The heliostats highlighted in red are those sequentially selected to be eliminated due to their low LCOE per unit area values. As expected, the number of large-size heliostats deleted increases as the heliostat cost per unit area of small size decreases and different solutions are obtained depending on the fixed scenario.

At each scenario, the algorithm stops when no improvement in the LCOE value is found. The results and final fields obtained using the *Expansion-Contraction Algorithm* are shown in Figures 6(a)-6(c) and Tables 3-4, where N_{dif} denotes the number of large-size heliostats deleted by the algorithm at each iteration.

The LCOE result obtained at the worst scenario (Table 3, Scenario-100) is similar to the reference plant **PS10**-592 and shows an improvement over Ω_0. In this scenario, the best field is obtained with Ω_5. In Table 4, the results obtained using Scenario-80 show a reduction of approximately 10% on the LCOE of the reference field. The best configuration is obtained with Ω_{12}.
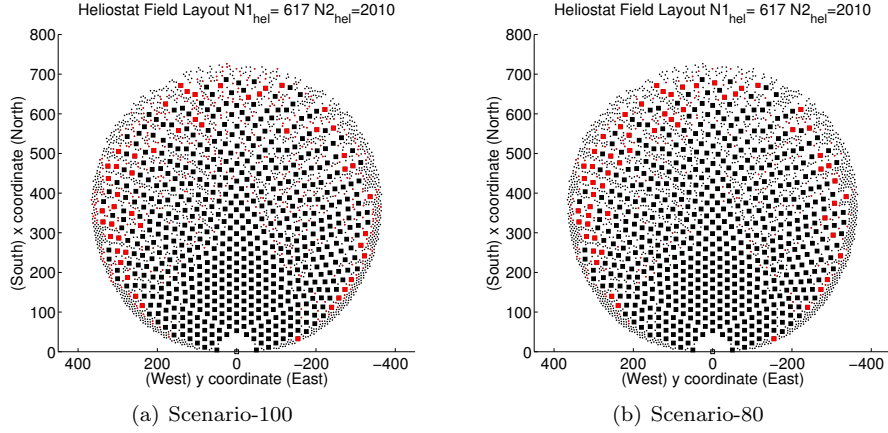
| | (a) Scenario-100 | (b) Scenario-80 |

Figure 5: Detail of *Expansion-Contraction* phases for Ω_0

For Scenario-80, a multi-size-heliostat field reaching better LCOE value than the reference field is obtained. Note that, with the same heliostats sizes, if we reduce the heliostat cost per unit area of small-size (for instance applying Scenario-60), multi-size-heliostat fields do not seem to be advantageous, as it is optimal to use heliostats of just one size.

Field	N	N_{small}	N_{large}	N_{dif}	$\Pi_{T_d}(\Omega)$	$E(\Omega)$	$F_{100}(\Omega)$
PS10-592	592	0	592	0	45.03	127.4	0.018153
Ω_0	617	0	617	0	45.06	126.0	0.018218
Ω_1	2077	1509	568	49	45.08	126.6	0.01822389
Ω_2	3265	2741	524	44	45.07	126.9	0.01818337
Ω_3	3737	3231	506	18	45.03	127.0	0.01817219
Ω_4	4005	3509	496	10	45.04	127.0	0.01816375
Ω_5	4138	3647	491	5	45.04	127.0	0.01815871
Ω_6	4191	3702	489	2	45.04	127.0	0.01815947

Table 3: Results Scenario-100. Π_t (MWth) and E (GWHth)

Ω_5 (Figure 6(a), Scenario-100) improves the LCOE value of the initial field Ω_0, and Ω_{12} (Figure 6(c), Scenario-80) improves also the LCOE value of the reference field **PS10**-592. These fields reach good LCOE values and attain the power requirement imposed.

As it can be seen in the resulting fields, there exist some holes and visual irregularities (due to heliostat(s) deleted at the last iterate and/or the nature of the problem: many local optima and non-convex constraints). In order to address these irregularities, the small-size heliostats can be directly relocated again, obtaining the regularized field Ω_5-R. However, the shading and blocking effects increase with this compactification and the annual energy value is reduced. In order to further improve the objective function, a pattern-free re-

Field	N	N_{small}	N_{large}	N_{dif}	$\Pi_{T_d}(\Omega)$	$E(\Omega)$	$F_{80}(\Omega)$
PS10-592	592	0	592	0	45.03	127.4	0.01815321
Ω_0	617	0	617	0	45.06	126.0	0.01821765
Ω_1	2359	1801	558	59	42.56	126.6	0.01797579
Ω_2	3991	3493	498	68	45.07	127.0	0.01769150
Ω_3	5670	5233	437	61	45.04	127.3	0.01742744
Ω_4	7361	6983	378	59	45.08	127.8	0.01719140
Ω_5	9094	8775	319	59	45.07	128.2	0.01698835
Ω_6	10822	10560	262	57	45.10	128.7	0.01681101
Ω_7	12077	11857	220	42	45.04	128.8	0.01670116
Ω_8	12763	12567	196	24	45.05	128.9	0.01661266
Ω_9	13201	13020	181	15	45.06	129.0	0.01655795
Ω_{10}	13358	13183	175	6	45.03	129.0	0.01653191
Ω_{11}	13455	13283	172	3	45.08	129.2	0.01650940
Ω_{12}	13493	13322	171	1	45.11	129.3	0.01650116
Ω_{13}	13526	13357	169	2	45.04	129.1	0.01650383

Table 4: Results Scenario-80. Π_t (MWth) and E (GWHth)

(a) Ω_5 Scenario-100

(b) Ω_5-R Scenario-100
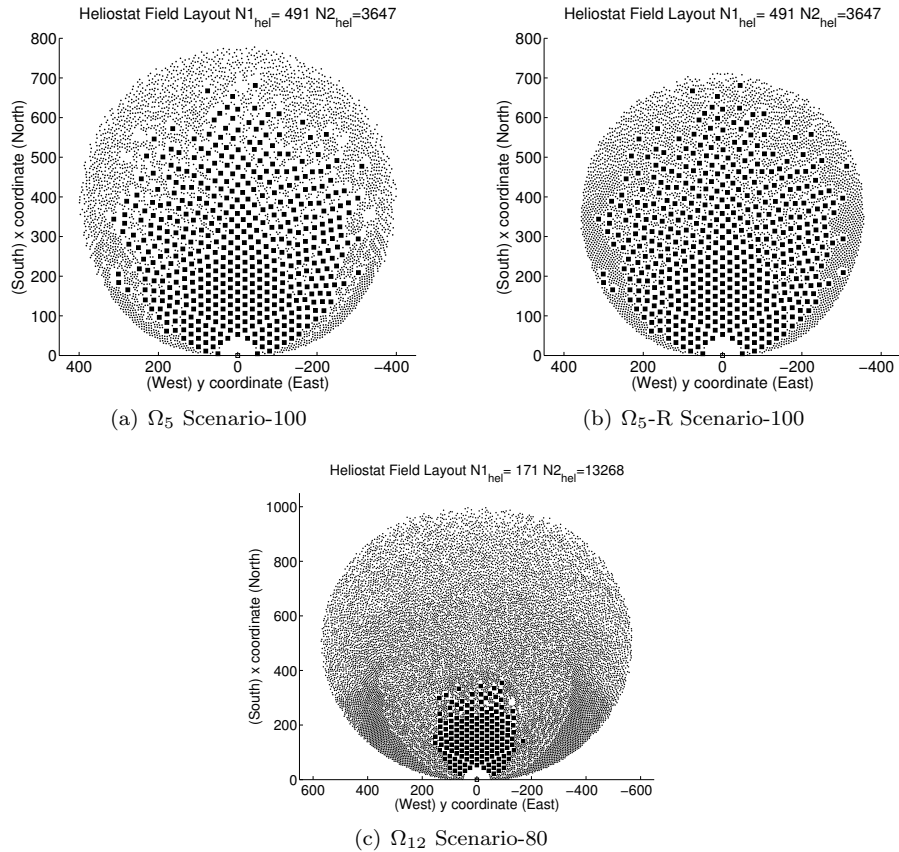

(c) Ω_{12} Scenario-80

Figure 6: Final Fields

13

finement procedure called "heliostat field improvement" can be applied, see [45].

With the selected heliostat sizes, tower-receiver configuration and power requirement, multi-size-heliostat fields with better LCOE values than the initial single-size-heliostat field are presented. The numerical experiments show the effects of combining heliostats of different sizes, according to various costs per unit area.

5. Concluding remarks and extensions

An algorithm for optimizing a multi-size-heliostat field has been proposed, in which both the location and the size of the heliostats are simultaneously considered. The algorithm tends to locate large-size heliostats in the most efficient regions of the field, and small-size heliostats (of the same cost/m^2), near the borders and to fill-in the holes between large sizes heliostats when advantageous. If the smaller heliostats have lower cost/m^2 then the algorithm tends to replace all the larger and more expensive ones.

Using the *Expansion-Contraction* algorithm, a detailed comparative study can be performed, taking into account the different heliostats sizes available at the time of building an SPT system (having different aspect ratio, cost per unit area, etc.), showing the usefulness of multi-size-heliostat or single-size-heliostat fields. Note that, following the proposed algorithm, different and more specific cost functions could be considered without modifying the method.

In this paper, the algorithm has been applied with two different heliostat sizes. However, following the idea of the procedure, heliostat fields with more than two heliostat sizes could also be generated.

For simplicity, we have considered that all the heliostats have the same height of elevation axis and, also, that the aiming point is unique. Considering different pedestal heights for each size (or even different heights for the same size) and also include an aiming strategy, are very interesting and difficult problems that need to be studied in the future.

The pattern-free location strategy used in this paper can be extended to successfully cover many other situations, as for instance ground irregularities, the effect of tower shading, variable (stochastic) meteorological data and multi-tower plants [46]. Note that the fields obtained with pattern-free strategies are less regular than the traditional pattern-based fields. However, new cleaning and maintenance strategies can be used for this kind of fields (see [47]) and, if necessary, road access can be directly included without modifying the algorithm.

In practice, not only the heliostat field but also the tower-receiver sub-system must be optimized. This can be done following an *Alternating* algorithm, as suggested in [33]. This algorithm consists of sequentially optimizing the field layout for a given tower-receiver design and, then, optimize the tower-receiver sub-system for the previously obtained field. This process is repeated until no improvement in the objective function is found.

6. Acknowledgements

[1] O. Behar, A. Khellaf, and K. Mohammedi. A review of studies on central receiver solar thermal power plants. *Renewable and Sustainable Energy Reviews*, 23:12–39, 2013.

[2] F. J. Collado and J. Guallar. A review of optimized design layouts for solar power tower plants with campo code. *Renewable and Sustainable Energy Reviews*, 20:142–154, 2013.

[3] V. S. Reddy, S. C. Kaushik, K. R. Ranjan, and S. K. Tyagi. State-of-the-art of solar thermal power plants- A review. *Renewable and Sustainable Energy Reviews*, 27:258–273, 2013.

[4] M. Romero, R. Buck, and J. E. Pacheco. An update on Solar Central Receiver Systems, Projects and Technologies. *Journal of Solar Energy Engineering*, 124:(11 Pages), 2002.

[5] A. Ramos and F. Ramos. Strategies in Tower Solar Power Plant optimization. *Solar Energy*, 86:2536–2548, 2012.

[6] F. J. Collado and J. Guallar. Campo: Generation of regular heliostat fields. *Renewable Energy*, 46:49–59, 2012.

[7] F.W. Lipps. Theory of Cellwise Optimization for Solar Central Receiver Systems. Technical Report SAND-85-8177, Houston Univ., TX (USA). Energy Lab., 1981. URL www.osti.gov/scitech/biblio/5734792.

[8] F. W. Lipps and L. L. Vant-Hull. A cellwise method for the optimization of large central receiver systems. *Solar Energy*, 20:505–516, 1978.

[9] F. M. F. Siala and M. E. Elayeb. Mathematical formulation of a graphical method for a no blocking heliostat field layout. *Renewable Energy*, 23:77–92, 2001.

[10] X. Wei, Z. Lu, Z. Wang, W. Yu, H. Zhang, and Z. Yao. A new method for the design of the heliostat field layout for solar tower power plant. *Renewable Energy*, 35(9):1970–1975, 2010.

[11] C. J. Noone, M. Torrilhon, and A. Mitsos. Heliostat field optimization: A new computationally efficient model and biomimetic layout. *Solar Energy*, 86:792–803, 2012.

[12] M. Sánchez and M. Romero. Methodology for generation of heliostat field layout in central receiver systems based on yearly normalized energy surfaces. *Solar Energy*, 80(7):861–874, 2006.

[13] P. Schramek and D. R. Mills. Heliostats for maximum ground coverage. *Energy*, 29:701–713, 2004.

[14] J. G. Kolb, S. A. Jones, M. W. Donnelly, D. Gorman, R. Thomas, R. Davenport, and R. Lumia. Heliostat Cost reduction study. Technical Report SAND2007-3293, Sandia National Labs., 2007. URL http://prod.sandia.gov/techlib/access-control.cgi/2007/073293.pdf.

[15] J. Göttsche, B. Hoffschmidt, S. Schmitz, M. Sauerborn, R. Buck, E. Teufel, K. Badstübner, D. Ifland, and C. Rebholz. Solar Concentrating Systems using Small Mirror Arrays. *Solar Energy Engineering*, 132:011003–011007, 2010.

[16] W. Landman. Sensitivity analysis of a curved heliostat profile. In *Proceedings of Annual Student Symposium 2012 in CRSES*, 2012.

[17] T. R. Mancini. Catalog of solar heliostats. Technical Report III–1/00, SolarPaces, 2000. URL www.fika.org/jb/resources/Heliostat%20Catalog.pdf.

[18] C. Zang, Z. Wang, H. Liu, and Y. Ruan. Experimental wind load model for heliostats. *Applied Energy*, 93:444–448, 2012.

[19] K. R. Bhargav, F. Gross, and P. Schramek. Life cycle cost optimized heliostat size for power towers. *Energy Procedia*, 49:40–49, 2014. SolarPaces 2013.

[20] J. B. Blackmon. Parametric determination of heliostat minimum cost per unit area. *Solar Energy*, 97:342–349, 2013.

[21] J. Coventry and J. Pye. Heliostat cost reduction – where to now? *Energy Procedia*, 49:60–70, 2014. SolarPaces 2013.

[22] L. Meng, Z. You, A. F. M. Arif, and S. Dubowsky. Shape optimized heliostats using a tailored stiffness approach. *Journal of Solar Energy Engineering*, 136(021017):(9 Pages), 2014.

[23] A. Pfahl. Survey of heliostat concepts for cost reduction. *Journal of Solar Energy Engineering*, 136(014501):1–9, 2014.

[24] G. García Navajas, A. Egea Gea, and M. Romero. Performance evaluation of the first solar tower operating with autonomous heliostats: PCHA project. In *Proceedings of the SolarPaces 2004*, 2004.

[25] A. Pfahl, M. Randt, C. Holze, and S. Untersch´utz. Autonomous lightweight heliostat with rim drives. *Solar Energy*, 92:230–240, 2013.

[26] A. Monreal, M. Burisch, M. Sanchez, D. Pérez, C. Villasante, E. Olabarrieta, D. Olasolo, and A. Olarra. EASY: An innovative design for cost effective heliostats/solar fields. *Energy Procedia*, 49:174–183, 2014. SolarPaces 2013.

[27] P. Ricklin, M. Slack, D. Rogers, and R. Huibregtse. Commercial readiness of esolar next generation heliostat. *Energy Procedia*, 49:201–208, 2014. SolarPaces 2013.

[28] A. Pfahl, M. Buselmeier, and M. Zaschke. Wind loads on heliostats and photovoltaic trackers of various aspect ratios. *Solar Energy*, 85:2185–2201, 2011.

[29] P. Schramek, D. R. Mills, W. Stein, and P. Le Livre. Design of the Heliostat Field of the CSIRO Solar Tower. *Journal of Solar Energy Engineering*, 131 (024505):(6 Pages), 2009.

[30] Solucar. 10 mw solar thermal power plant for southern spain. Technical report, Solucar, Inabensa, Fichtner, CIEMAT and DLR, 2006. URL http://www.trec-uk.org.uk/reports/ps10_final_report.pdf.

[31] M. Renzi, C. M. Bartolini, M. Santolini, and A. Arteconi. Efficiency assessment for a small heliostat solar concentration plant. *International Journal of Energy Research*, 39:265–278, 2015.

[32] L. Crespo, F. Ramos, and F. Martínez. Questions and answers on solar central receiver plant design by NSPOC. In *Proceedings of SolarPaces 2011*, 2011.

[33] E. Carrizosa, C. Domínguez-Bravo, E. Fernández-Cara, and M. Quero. A heuristic method for simultaneous tower and pattern-free field optimization on solar power systems. *Computers & Operations Research*, 57:109–122, 2015.

[34] F. Biggs and C.N. Vittitoe. The HELIOS model for the optical behavior of reflecting solar concentrators. Technical Report SAND76–0347, Sandia National Labs., 1976. URL http://prod.sandia.gov/techlib/access-control.cgi/1976/760347.pdf.

[35] F. J. Collado and J.A. Turégano. Calculation of the annual thermal energy supplied by a defined heliostat field. *Solar Energy*, 42:149–165, 1989.

[36] G. Sassi. Some notes on shadow and blockage effects. *Solar Energy*, 31(3): 331–333, 1983.

[37] F. J. Collado and J.A. Turégano. An analytic function for the flux density due to sunlight reflected from a heliostat. *Solar Energy*, 37:215–234, 1986.

[38] L. Crespo and F. Ramos. NSPOC: A New Powerful Tool for Heliostat Field Layout and Receiver Geometry Optimizations. In *Proceedings of SolarPaces 2009*, 2009.

[39] F. J. Collado. One point fitting of the flux density produced by a heliostat. *Solar Energy*, 84:673–684, 2010.

[40] F. W. Lipps. Four different views of the Heliostat Flux Density Integral. *Solar Energy*, 18:555–560, 1976.

[41] E. Carrizosa, C. Domínguez-Bravo, E. Fernández-Cara, and M. Quero. Optimization of multiple receivers solar power tower systems. *Energy*, 90: 2085–2093, 2015.

[42] M. Ergen, C. Coleri, and P. Varaiya. Qos aware adaptative resource allocation techniques for fair scheduling in OFDMA based broadband wireless access systems. *IEEE Transactions on Broadcasting*, 49:362–370, 2003.

[43] Fichtner. Assessment of technology options for development of concentrating solar power in south africa for the world bank. In *The Climate Investment Funds*, 2010. URL https://www-cif. climateinvestmentfunds.org/sites/default/files/Presentation% 20-%20WB%20(Eskom)%20Project%20-%202010_12_07%20.pdf.

[44] R. Osuna, V. Fernández, S. Romero, M. Romero, and M. Sánchez. PS10: a 11.0-MWe Solar Tower Power Plant with Satured Steam Receiver. In *Proceedings of SolarPaces 2004*, 2004.

[45] R. Buck. Heliostat field layout improvement by nonrestricted refinement. *Journal of Solar Energy Engineering*, 136(021014):(6 Pages), 2014.

[46] P. Schramek and D. R. Mills. Multi-tower solar array. *Solar Energy*, 75(3): 249–260, 2003.

[47] L. Alon, G. Ravikovich, M. Mandelbrod, U. Eilat, Z. Schop, and D. Tamari. Computer-based management of mirror-washing in utility-scale solar thermal plants. In *Proceedings of ASME 2014 (8th International Conference on Energy Sustainability and 12th International Conference on Fuel Cell Science, Engineering and Technology)*, volume 1, July 2014.